Interlaboratory Comparison of Traceable Atomic Force Microscope Pitch Measurements

Ronald Dixson[1], Donald A. Chernoff[2], Shihua Wang[3], Theodore V. Vorburger[1],
Siew Leng Tan[3], Ndubuisi G. Orji[1], Joseph Fu[1]

[1]National Institute of Standards and Technology, 100 Bureau Drive Stop 8212, Gaithersburg, MD 20899
[2]Advanced Surface Microscopy, 3250 N. Post Rd., Ste. 120, Indianapolis, IN 46226
[3]National Metrology Centre, A*STAR, 1 Science Park Dr. Singapore 118221

ABSTRACT

The National Institute of Standards and Technology (NIST), Advanced Surface Microscopy (ASM), and the National Metrology Centre (NMC) of the Agency for Science, Technology, and Research (A*STAR) in Singapore have completed a three-way interlaboratory comparison of traceable pitch measurements using atomic force microscopy (AFM). The specimen being used for this comparison is provided by ASM and consists of SiO_2 lines having a 70 nm pitch patterned on a silicon substrate.

NIST has a multifaceted program in atomic force microscope (AFM) dimensional metrology. One component of this effort is a custom in-house metrology AFM, called the calibrated AFM (C-AFM). The NIST C-AFM has displacement metrology for all three axes traceable to the 633 nm wavelength of the iodine-stabilized He-Ne laser – a recommended wavelength for realization of the SI (*Système International d'Unités,* or International System of Units) meter. NIST used the C-AFM to participate in this comparison.

ASM used a commercially available AFM with an open-loop scanner, calibrated by a 144 nm pitch transfer standard. In a prior collaboration with Physikalisch-Technische Bundesanstalt (PTB), the German national metrology institute, ASM's transfer standard was calibrated using PTB's traceable optical diffractometry instrument. Thus, ASM's measurements are also traceable to the SI meter.

NMC/A*STAR used a large scanning range metrological atomic force microscope (LRM-AFM). The LRM-AFM integrates an AFM scanning head into a nano-stage equipped with three built-in He-Ne laser interferometers so that its measurement related to the motion on all three axes is directly traceable to the SI meter.

The measurements for this interlaboratory comparison have been completed and the results are in agreement within their expanded uncertainties and at the level of a few parts in 10^4.

Keywords: AFM, metrology, pitch, standards, calibration, traceability

1. INTRODUCTION

Traceable pitch standards (gratings) are commonly used to calibrate the magnification of scanning electron microscopes (SEMs) and atomic force microscopes (AFMs) in the *x-y* plane. Structures with critical dimensions smaller than 100 nm already exist in semiconductor and data storage products and are produced for research in other areas of nanotechnology, including optics and medicine. The availability of traceable gratings with pitch smaller than 100 nm will enable more accurate measurement of such structures for the simple reason that a microscopic image 100 nm wide cannot be calibrated by a grating whose pitch is much larger than 70 nm. This paper compares traceable pitch measurements made in three different laboratories using three different AFMs on the same 70 nm pitch grating.

Since the details of edge bias and other shape distortions that result from the probe-sample interaction generally cancel out in a pitch (feature spacing) measurement, pitch is a measurand that is largely insensitive to the type of instrument

Scanning Microscopy 2010, edited by Michael T. Postek, Dale E. Newbury, S. Frank Platek, David C. Joy,
Proc. of SPIE Vol. 7729, 77290M · © 2010 SPIE · CCC code: 0277-786X/10/$18 · doi: 10.1117/12.858353

being used (e.g., AFM, SEM, optical microscope). Therefore, the results presented here have applicability to instruments other than AFMs, such as SEMs and optical instruments.

The participants in this interlaboratory comparison were the National Institute of Standards and Technology (NIST), Advanced Surface Microscopy (ASM), and the National Metrology Centre (NMC) of the Agency for Science, Technology, and Research (A*STAR) in Singapore. The specimen being used for this comparison was provided by ASM and consists of SiO_2 lines having a 70 nm pitch patterned on a silicon substrate.

NIST used a custom in-house dimensional metrology AFM, called the calibrated AFM (C-AFM). [1] The NIST C-AFM incorporates interferometric displacement metrology in all three axes to achieve traceability to the SI (*Système International d'Unités,* or International System of Units) meter. ASM used a commercially available AFM with an open-loop scanner, calibrated by a 144 nm pitch transfer standard. In a prior collaboration with Physikalisch-Technische Bundesanstalt (PTB), the German national metrology institute, ASM's transfer standard was calibrated using PTB's traceable optical diffractometry instrument. Thus, ASM's measurements are also traceable to the SI meter. [2] NMC/A*STAR used a large scanning range metrological atomic force microscope (LRM-AFM). [3] The LRM-AFM integrates an AFM scanning head into a nano-positioning stage equipped with three built-in He-Ne laser interferometers so that displacements in all three axes are directly traceable to the SI meter.

In this paper, we describe the instruments and methods used in each lab, the specimen and sampling plan, and the results of the comparison including the uncertainty estimates.

2. INSTRUMENTS AND METHODS USED FOR MEASUREMENTS

2.1 The NIST Calibrated Atomic Force Microscope (C-AFM)

The NIST C-AFM was constructed to perform traceable dimensional metrology. It is intended primarily to calibrate physical standards for other AFMs. The design, performance, and uncertainties of the system have been discussed elsewhere [1,4-6]. The C-AFM has metrology traceability to the SI meter in all three axes via the 633 nm wavelength of an I_2-stabilized He-Ne laser. The lateral axes are controlled closed-loop using interferometry. The *z*-axis uses a capacitance gauge for real time displacement metrology, and this cap gauge is calibrated off-line using interferometry. The C-AFM operates in contact mode and performs both pitch and step height measurements.

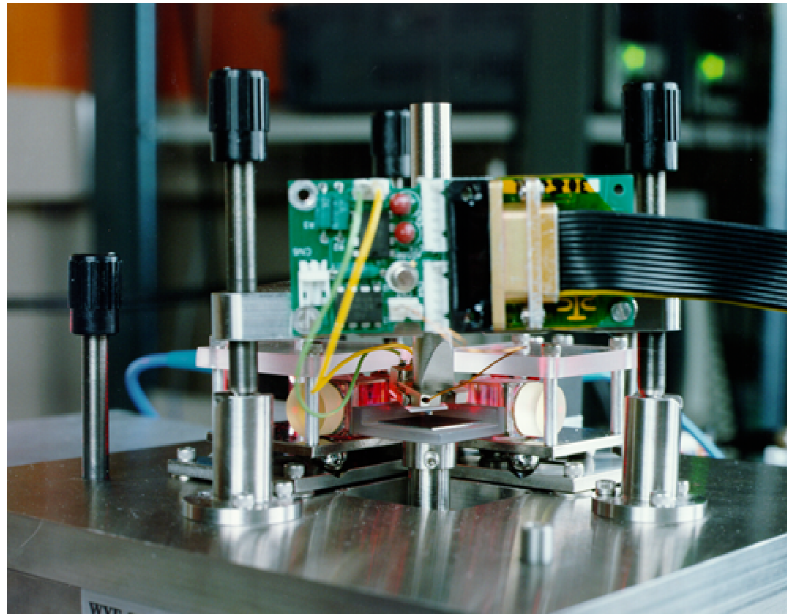

Figure 1. Side view of the NIST C-AFM – showing the head and metrology frame.

A scanning sample design was chosen for the C-AFM, largely for the ease of interferometry integration with low Abbe offsets – a few millimetres in this case. A photograph of the C-AFM metrology frame and head is shown in Fig. 1. The composite scanner consists of an *x*-*y* flexure stage and an independent *z*-stage with an integrated capacitance sensor to which the specimen platform is attached. This scanner displaces the specimen platform relative to the metrology frame. Both the lateral interferometer optics and the AFM head are mounted kinematically to the metrology frame. This design permits the lateral axis interferometry to be done real time, allowing the option of closed-loop position control in the lateral axes.

The stage is supplied with a stand alone programmable digital controller that allows for closed-loop operation using the integrated capacitance sensors. Since we use interferometers and our AFM scan controller to independently close the loop, we operate the stage itself open-loop with respect to the capacitance gauges for the *x* and *y* axes. However, by using the closed loop control for the other four degrees of freedom, we are able to reduce the undesired angular motion of the stage and the resulting lateral axis Abbe errors by three orders of magnitude relative to prior generations of the instrument. [4,6] We were also able to reduce the out-of-plane motion error (i.e., the *z*-straightness of the *x* and *y* axes) to less than 1 nm over the almost 100 µm lateral scan range.

2.2 Characterized commercial AFM at ASM

ASM used a Veeco Metrology/Digital Instruments Dimension 3100 AFM[†], operated by a NanoScope® IIIA controller with Electronics extender module (“phase box”). The open-loop scanner was calibrated to factory specifications. During measurements, the tip is scanning and the sample is stationary. Large and/or massive samples can be examined, as can be seen in Fig. 2. The AFM can operate in TappingMode™ or contact mode and the two modes give similar precision. One run in each mode was performed in this work. The images produced by the open-loop scanner are calibrated using images of a 144 nm pitch transfer standard. In a prior collaboration with Physikalisch-Technische Bundesanstalt (PTB), the German national metrology institute, ASM’s transfer standard was calibrated using PTB’s traceable optical diffractometry instrument. Thus, ASM’s measurements are also traceable to the SI meter. [2]

Figure 2. Dimension 3100 AFM at ASM, showing the scanner and a large test specimen.

[†]Certain commercial equipment is identified in this paper to adequately describe the experimental procedure. Such identification does not imply recommendation or endorsement by the National Institute of Standards and Technology nor does it imply that the equipment identified is necessarily the best available for the purpose.

An open-loop scanner has the potential advantage that its images are not affected by the sensor noise present in closed-loop systems, but it has the real disadvantage that piezoelectric actuators suffer from nonlinearity and other faults. Although the NanoScope controller corrects for most of the piezoscanner nonlinearity in real time, residual nonlinearity means that pitch values measured at the edge of an image can differ by 5 % from the average value. In addition, the average magnification can change by 1 % to 3 % during a day. These unfavorable characteristics are overcome here by ASM's data capture and analysis protocols. Both the 70 nm pitch test specimen and the 144 nm pitch transfer standard were placed on the sample stage at the same time and image capture alternated between them. During data analysis, each test image was calibrated using the preceding and following images of the transfer standard, a procedure which automatically corrects for short term calibration drift. Further details are given in the section 4.

2.3 Traceable Metrology AFM at NMC/ASTAR

NMC/A*STAR is using a large scanning range metrological atomic force microscope (LRM-AFM). [3] The LRM-AFM, shown in Fig. 3, integrates an AFM scanning head into a nano-stage equipped with three built-in He-Ne laser interferometers so that its measurement related to the motion on all three axes is directly traceable to the SI meter.

The LRM-AFM consists of an AFM probe, a Nano Measuring Machine (NMM), control electronics and software for coordinating servo motion control, signal detection, data acquisition and analysis. An isolation table and an acoustical enclosure are also furnished to minimize the influence of external vibration and noise on the system's performance. The AFM, which is capable of working in non-contact mode, was integrated into the NMM. The motions along the three co-ordinate axes of the NMM were measured by three stabilized He-Ne laser interferometers. The laser frequencies were calibrated by an iodine frequency stabilized laser.

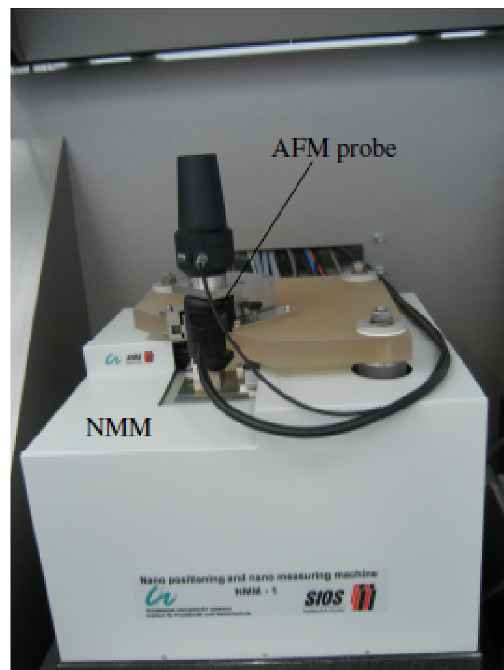

Figure 3. Photograph of the LRM-AFM at NMC/A*STAR in Singapore.

3. SPECIMEN AND SAMPLING METHOD

3.1 70 nm Pitch Specimen

A commercially available 70 nm pitch standard, Model 70-1DUTC (serial number 3555K203) supplied by ASM, was chosen for this comparison. The specimen, a 3 mm × 4 mm silicon chip with ridges of silicon oxide, is mounted on

steel disk for convenience, as shown in Fig. 4 below. The array of ridges covers an area 1.2 mm × 0.5 mm, near the center of the 4 mm × 3 mm chip. The ridge height and width are approximately 35 nm, but these are not the calibrated dimensions. Only the pitch is calibrated. Eleven measurement locations were distributed across the central patterned area of the specimen. A typical AFM scan of this specimen is shown in Fig. 5.

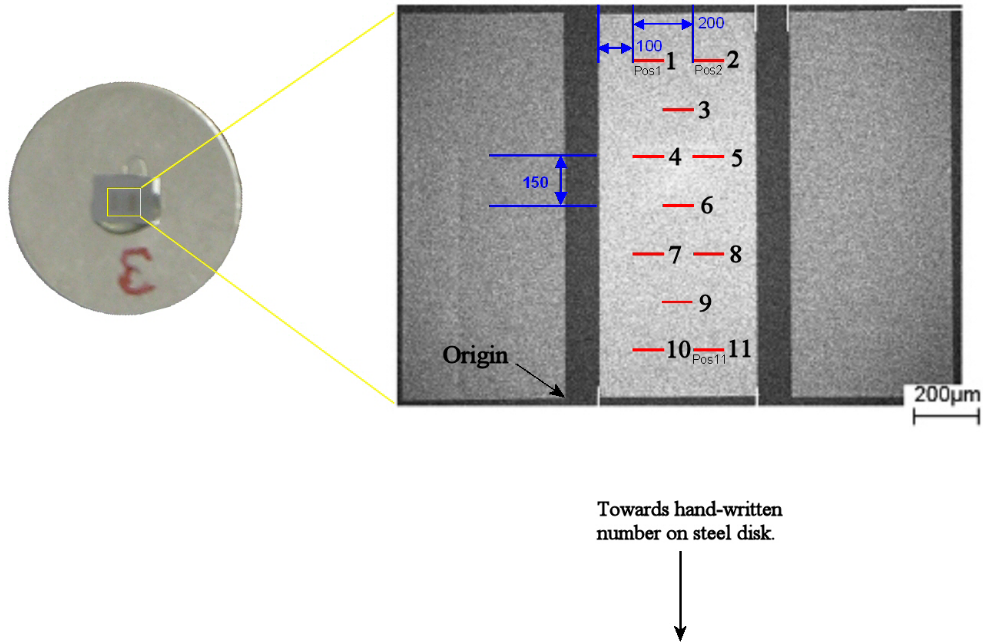

Figure 4. Picture and layout of sampling plan on 70 nm pitch grating. All dimensions are in μm.

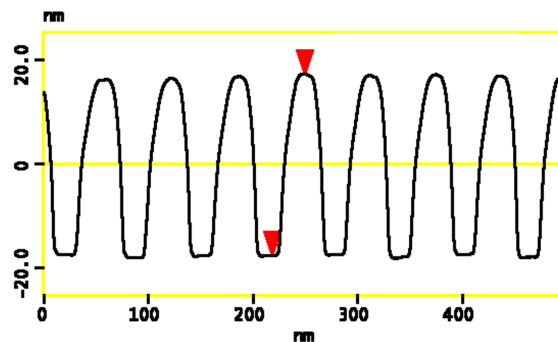

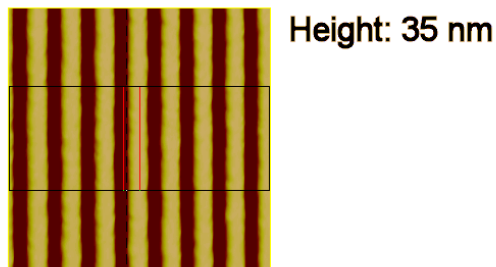

Figure 5. AFM height image and average profile of the 70 nm pitch standard.

The sampling plan shown in Fig. 4 was used as a guide by the participants, with each laboratory attempting to measure as close to the target location as possible, but avoiding defects as necessary. Each laboratory chose the scanning conditions and image size, and analysis methods depending on the specific strengths of their instruments.

NIST used an image size of 50 µm × 50 µm with 256 scan lines and 4000 points along the fast scan axis; the average data sampling interval was thus 12.5 nm. All data were obtained using contact mode imaging. The analysis used was a frequency domain method in which the peak of the power spectral density is located for each scan line used. The mean pitch for each scan line is then determined from the average peak location.

ASM used 3 µm × 3 µm square images with 512 × 512 pixels; the data sampling interval was thus 5.9 nm. The analysis used was a real-space method that extracts the pitch of each interval in the image. Pitch data from the calibration scans that preceded and followed each measurement image of the 70 nm grating were used to correct the pitch results for the comparison specimen. This method mitigates the potential impact of any drift in scale calibration. Individual pitch values are reported for each pair of consecutive ridges in the image. One measurement run used contact mode and one used TappingMode™.

NMC/A*STAR used a measurement area of 100 µm × 100 µm at each spot. The images were obtained using intermittent contact mode. The fast scan direction was orthogonal to the ribs of the gratings and the slow axis spacing between profiles was 10 µm. 50 000 data points were captured for each profile; the data sampling interval was thus 2 nm. The measurement data were evaluated using a Fast Fourier Transform method to determine the mean pitch over an effective scanning range of 80 µm.

For all three labs, the final measurement result is the grand average of all the average values obtained from the eleven different measurement positions on the sample.

4. RESULTS OF COMPARISON

The overall average pitch values and expanded uncertainties obtained by the participants are shown in Table I, and Fig. 6 shows the average pitch values at each of the eleven measurement locations.

Table I. Mean pitch values obtained from four measurement runs at three labs, shown in chronological order.

Run	Mean Pitch (nm)	Expanded Uncertainty (nm) (k = 2)
ASM#1	70.071	0.024
NMC	70.072	0.028
NIST	70.055	0.027
ASM#2	70.090	0.021
ASM combined	70.080	0.016

The standard approach [7,8] to uncertainty budgets adopted by National Metrology Institutes (NMIs) such as NIST and NMC/A*STAR is to develop an estimated contribution for every known source of uncertainty in a given measurement and to include terms pertaining to both the instrument used and the particular specimen measured. Terms evaluated exclusively by statistical methods are known as type A components. Terms evaluated using some combination of measured data, physical models, or assumptions about the probability distribution are known as Type B components.

This approach was used for our inter-laboratory comparison, with each laboratory developing a draft analysis and uncertainty statement for its own results and then reviewing this analysis with the other participants before publication. In each case, a complete table of uncertainty components is presented, but only the three largest components are discussed in detail.

4.1 NIST C-AFM Results

NIST measured the specimen in Oct. 2009 and obtained an average pitch of 70.055 nm ± 0.027 nm ($k = 2$). The NIST C-AFM images were all 50 µm in scan size and were obtained in contact mode. One image was obtained at each location, except for location 2, where a second image was taken to help assess instrument repeatability. The data set thus includes sampling of grating non-uniformity and instrument repeatability. Due to particulate contamination at the originally intended location 1, the actual measurement site was moved approximately 100 µm in the direction of location 4.

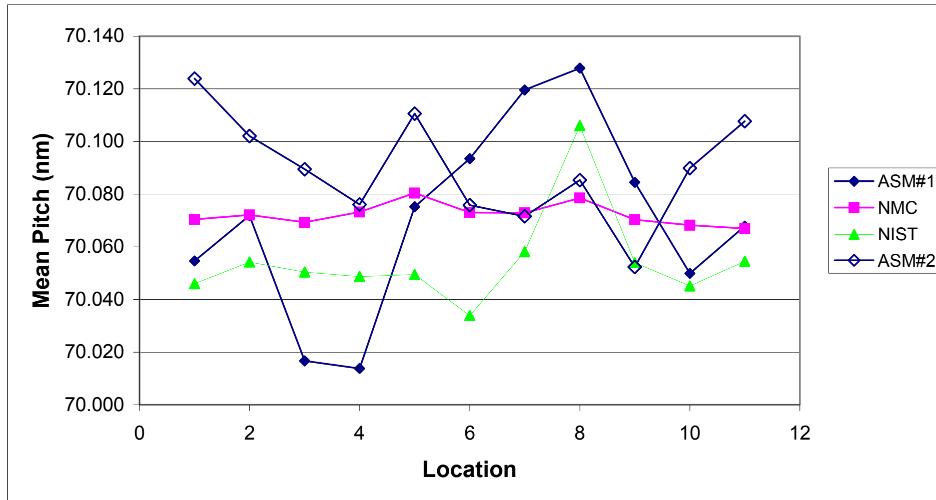

Figure 6. Mean pitch value of the 70 nm standard by spot, obtained from four measurement runs.

For each image, the pitch was determined using a frequency domain analysis. An in-house program written in the PV-Wave data analysis language was used to locate the relevant peak in the power spectral density (PSD). The analysis was performed line by line and the results are then averaged for all of the profiles in an image. The average pitch at each of the eleven locations was shown in Fig. 6. The grand average is given in table II.

Table II. Summary of C-AFM pitch results on the 70-1DUTC grating SN203.

Average Pitch:	70.05458 nm
Standard Deviation of Eleven Locations:	0.018239 nm
Standard Deviation of the Mean:	0.0055 nm

The estimated value of the measurand is the average of these eleven results, 70.0546 nm. The type A uncertainty, evaluated from the measurements, includes instrument repeatability and reproducibility as well as the effect of sample non-uniformity. It was calculated from the standard deviation of the mean (SDOM) of all eleven results, 0.0055 nm.

4.1.1 Type B Uncertainties in C-AFM Pitch Measurements

The type B uncertainties arise from several different sources and were evaluated by various methods. Some of the effects may depend on the sample and on the measurement strategy, such as the number of intervals or locations measured. Three of the type B components listed as potential uncertainties in Table III are shown as zero. This is because we consider them to be negligible uncertainties in this particular case, but not necessarily in all cases. These effects must be evaluated for each measurement on a case by case basis.

In general, the sources of uncertainty in C-AFM measurements have been previously discussed. [4,6] Therefore, for brevity, only the three largest components are discussed here. These are the type A contribution from sample non-

uniformity and repeatability – which was discussed in the previous section – the algorithm uncertainty, and the in-plane cosine error.

The first component listed in the type B budget is for the algorithm and measurand definition. For this term, we considered how closely the calculated result, the value calculated from the apparent location of the appropriate peak in the frequency domain, corresponds to the intended measurand of average pitch – as would be determined from the actual location of the peak.

The 70-1DUTC grating specimen has a high level of uniformity across the grating. It is intended for use in scanned probe microscopes (SPMs) and scanning electron microscopes (SEMs) as a scale calibration reference. Therefore, we regard a frequency domain analysis method – which involves averaging over a significant number of intervals – to be the most relevant for this application, and this was the main focus of our analysis.

Table III. C-AFM Pitch Uncertainty Budget for 70 nm pitch measurement

Component	Relative Standard Uncertainty (proportional contributions)	Standard Uncertainty (nm)
Type A		
Repeatability, Sample Variation (Standard Deviation of Mean of Eleven Measured Sites)		0.005499
Type B		
Algorithm/Measurand Definition		0.0065
Laser Interferometer, Digital Resolution		0.0 (*included in Type A due to averaging*)
Laser Interferometer, Polarization Mixing		0.0 (*included in Type A due to averaging*)
Laser Wavelength in Vacuum	1.0×10^{-7}	0.000007
Refractive Index of Air (Temperature, Pressure, Humidity)	5.1×10^{-6}	0.000357
Deformation/Damage of Tip		0.0 (*included in Type A due to averaging*)
Abbe Error Due to Rotation Around z-axis	2.0×10^{-6}	0.00014
Abbe Error Due to Rotation Around y-axis	2.5×10^{-5}	0.00175
Cosine Errors (in-sample-plane)	1.5×10^{-4}	0.0105
Cosine Errors (out-of-sample-plane)	1.5×10^{-6}	0.000105
Temperature Stability (thermal expansion)	7.6×10^{-7}	0.00005320
	Combined Standard Uncertainty (k = 1) :	0.0136
	Expanded Uncertainty (k = 2) :	0.0273

For the measurement, the centroid of the PSD peak was calculated using five points centered around the maximum. To estimate the type B uncertainty, the centroids were calculated using one through nine points. The differences observed between the one and nine point calculations were taken to represent extreme results and were used to determine the width of a rectangular distribution that describes the uncertainty associated with this method.

Additionally, for this measurement, the centroids were calculated using a threshold exclusion method to mitigate the contribution of any bad scan lines. The strongest peak was found, and only those scan lines with peak strength above a threshold fraction of this strongest peak were included. Reported results were obtained using 0.5 as the threshold, but the calculation was also performed using 0.25 and 0.75. These results were then taken as the width of the rectangular distribution that describes this contribution to the uncertainty. The standard uncertainties obtained from these two distributions were then added in quadrature to obtain the algorithm standard uncertainty component of 0.0065 nm.

The cosine error uncertainties arise from the potential for misalignments among the sample, scanner, and measurement axes. Since misalignments are possible in both the plane of the sample and out of it, we have divided this uncertainty into two terms. Cosine errors for a misalignment in θ approach zero as $\theta^2/2$, so these sources of uncertainty are normally manageable – especially since it is usually possible to estimate the misalignment angle (and correct the result) from the data to an uncertainty of 0.1° or less – which would correspond to an uncertainty of $1.5 \times 10^{-6} P$ in the measured pitch.

For these measurements, however, the low contrast images increased the difficulty of estimating the misalignment angle. Although direct estimation appeared successful for some images, most could not be corrected to the typical 0.1° level. Consequently, we relied on the more conservative estimate of 1° misalignment – which roughly corresponds to what is achievable when aligning the sample with the naked eye. As a result, the in-plane cosine error of $1.5 \times 10^{-4} P$ turned out to be the largest uncertainty contribution. Although this was a disappointing outcome for the present measurements, this source of uncertainty should be readily reducible in similar measurements or future extensions of this work.

4.2 ASM Results

ASM measured the specimen in two independent runs – one in contact mode (July 2009) and one in tapping mode (Nov. 2009). The final results for average pitch values were 70.071 nm and 70.090 nm, with expanded uncertainties ($k = 2$) of 0.024 nm and 0.021 nm, respectively. The difference between runs was not statistically significant. The overall average of both runs was 70.080 nm, with expanded uncertainty of 0.016 nm.

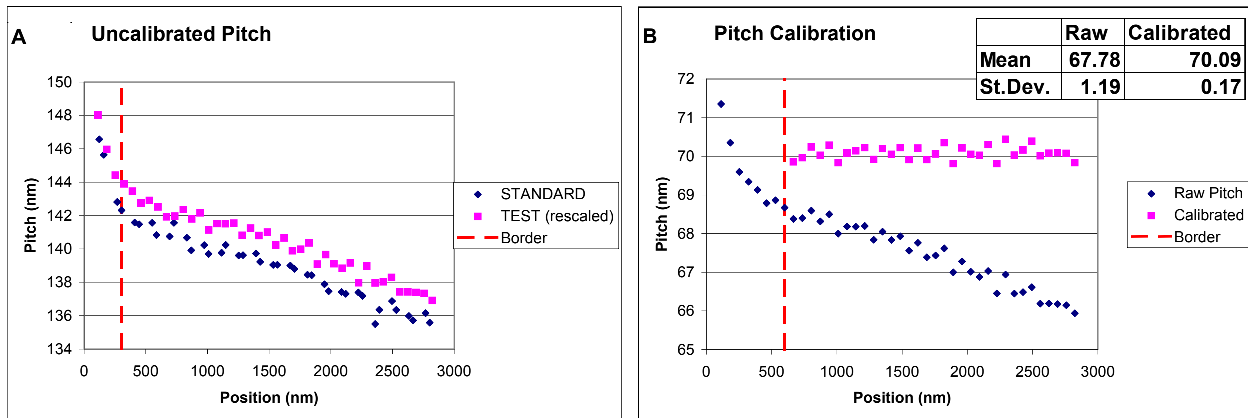

Figure 7. Pitch results for one data set. A: Raw pitch as a function of position in the image. Points labeled "Standard" are pitch values measured in the calibration images captured before and after the test specimen image. Points labeled "TEST (rescaled)" are pitch values from the test image, which were then multiplied by 2.0535 and offset by 1.5 nm for this graph. The two curves were approximately parallel. B: Raw and calibrated pitch for the test specimen. The dashed vertical lines indicate data exclusion borders. Because the AFM nonlinearity is hard to correct at the start of scan, we exclude pitch results from the leftmost 20 % of the test image and from the leftmost 10 % of the calibration images.

In order to appreciate that an open loop AFM can produce accurate results and to estimate the uncertainty, it is necessary to look in detail at the data analysis, where we will see that the most important uncertainty component is the

random variation of individual pitch values. The height contrast AFM images were analyzed using ASM's DiscTrack Plus™ and other software. In a given run of the software, we calculate the pitch using one measured image of the test specimen and two measured images of the calibration standard, one captured before and one captured after the test image. This procedure ("interleaved calibration") increases accuracy by correcting for short term drift in the AFM's magnification and it increases precision by using redundant calibration data.

The measurements were made according to procedures described in detail elsewhere [9-11] and summarized here. The software computes an average height profile Z(x) by averaging all scan lines. Peaks on the height profile correspond to ridges (for the 70 nm test specimen) or columns of bumps (for the 144 nm transfer standard). The centroid of each peak is its position. The difference of successive positions is an individual pitch value. No microscope is perfect and Fig. 7A shows there is a significant non-linearity in the image: apparent pitch values are large at the left side of the image (start of scan) and decrease towards the right. Because the image distortion is reproducible from one scan to the next, one can correct this systematic effect in the offline analysis. Using a 5th-order polynomial fit of pitch vs. position in the calibration images, the software computes a new length scale that corrects for average magnification error and non-linearity. The corrected length scale is then applied to the feature position data from the test image to produce a set of corrected pitch values. For this data set, calibration reduced the standard deviation by almost ×7 and removed a bias of 3.2 % in the mean value (see inset table in the figure).

Fig. 8 shows detailed results by spot in each of ASM's two runs. Because the data analysis is done in real space, each measurement is a single instance of pitch. Thus, the standard deviation given for each spot refers to single pitch measurements. At each spot, we measured about 34 single pitch values. The pooled standard deviations of single pitch values were 0.20 nm and 0.15 nm for runs 1 and 2, which used contact mode and TappingMode™, respectively.

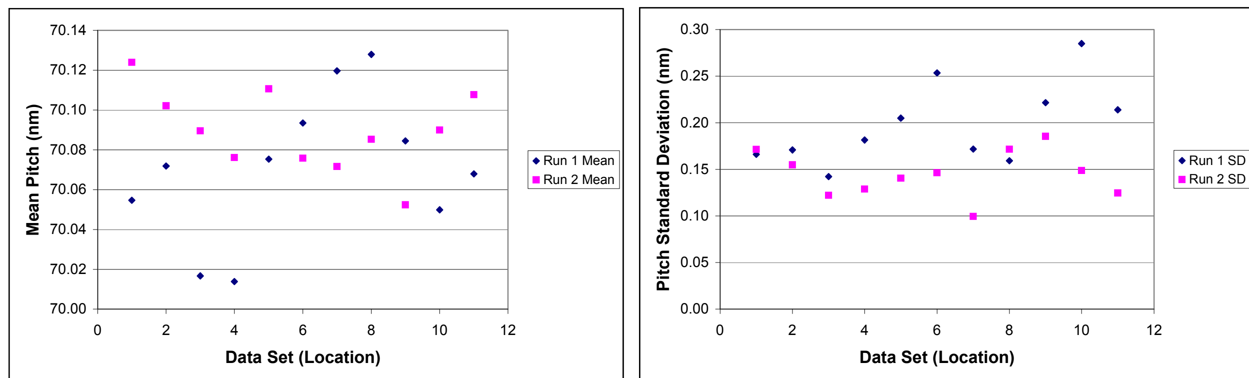

Figure 8. Mean pitch and standard deviation of single pitch values in two runs. Each data set corresponds to a specific location in the patterned area, but the very small scan size means it is very unlikely that corresponding scans in the two runs actually overlapped.

4.2.1 Uncertainties in ASM Measurements

The expanded uncertainty of single pitch (individual interval) values was 0.40 and 0.29 nm for runs 1 and 2, respectively. This uncertainty was dominated by the standard deviation of measured values, which accounted for more than 99 % of the overall variance. Note that the uncertainty of individual intervals is of interest to ASM but is much larger than the uncertainty of the average pitch – which was the measurand for this comparison. The uncertainty of single pitch values is thus not discussed further. The uncertainty components of the overall mean value and combined expanded uncertainties for the two ASM measurement runs are shown in table IV, where they are listed approximately in decreasing order of importance.

Magnification error and image nonlinearity are by far the largest errors present in the original data. We used an Analysis of Variance (ANOVA) [12] calculation to partition the overall variation into two components, called the "within group" and "between group" variances. A natural grouping of the data is by location. Then, the "within group" variance is the variance of individual pitch values at each location relative to the mean value there, averaged over all locations. The "between group" variance refers to the variance of mean pitch values for each location relative to the

overall mean. The ANOVA result showed that there was no statistically significant difference between images in each run. This is consistent with the impression of random variation given by the graph of mean pitch values in fig. 8. This means that the interleaved calibration method has successfully corrected for average magnification error. The random variation of pitch values vs. position within each image, as shown in fig. 7B, indicates that the length scale correction method has successfully corrected for the image nonlinearity. Therefore, we have corrected these effects as fully as is reasonably possible. The remaining random effects contained in the standard deviation of the mean include surface and edge roughness, local pitch variation in the test specimen (whether intrinsic or due to debris on the surface), error in the corrected length scale, tip shape changes and AFM noise.

Table IV. ASM's Pitch Uncertainty Budget for 70-1DUTC (k = 1)

Component	Standard Uncertainty (nm)					
	Run 1	Run 2	Both Runs	Variance (pm^2)	Relative Variance	Rank
SD of overall mean	0.0104	0.0076	0.0091	83.1	65.6%	1
Cosine factor for rotation in plane (0° to 1°) (relative uncertainty 6.5×10^{-5})	0.0046	0.0046	0.0046	20.7	16.3%	2
Pitch uncertainty of 144 nm standard (standard uncertainty = 0.0075 nm), (relative uncertainty 5.2×10^{-5})	0.0036	0.0036	0.0036	13.3	10.5%	3
Image Drift (relative standard uncertainty 1.7×10^{-5} and 5.6×10^{-5}) (depends on scan speed)	0.0012	0.0039	0.0029	8.3	6.5%	4
Cosine factor for out of plane tilt (0°to 0.5°) (relative uncertainty 1.6×10^{-5})	0.0011	0.0011	0.0011	1.3	1.0%	5
Combined Standard Uncertainty (nm)	0.01204	0.0104	0.0113	126.7	100.0%	
Expanded uncertainty, k = 2	0.0241	0.0208	0.0225 nm			
Expanded uncertainty, k = 2 for mean of 2 runs			0.0159 nm			

The Type B error of specimen rotation in plane is next in importance after the standard deviation of mean. We controlled the rotation of each specimen so that the grating axes were perpendicular to the fast scan direction within 1°. Our fundamental measurement is the ratio of the pitch of the test specimen to the pitch of the calibration standard. Rotation of the calibration standard decreases, and rotation of the test specimen increases, the reported pitch of the test specimen. The effect of rotation is proportional to a quotient of cosines, cos(A)/cos(B). With the assumption that the angles A and B have a rectangular distribution in the range -1 to +1°, then the mean of the quotient is 1.0 and the standard deviation of the quotient is 0.000065. This effect gives a constant bias within a given run and contributes to a run to run reproducibility error when specimens are replaced. The relative standard uncertainty of the run to run error is 6.5×10^{-5}.

The third most important component of uncertainty is the stated uncertainty of the mean pitch of the transfer standard (150-2DUTC, 0.0075 nm, 0.0052 %, k = 1), calibrated by optical diffraction at PTB.

4.3 NMC/A*STAR Results

NMC/A*STAR measured the specimen in Aug. 2009 and obtained an average pitch of 70.072 nm ± 0.028 nm (k = 2). The NMC/A*STAR data were analyzed using a frequency domain method for each profile at all eleven locations. The results are summarized in table V below.

Table V. Summary of the LRM-AFM measurements at NMC/A*STAR.

Average Pitch:	70.0723 nm
Standard Deviation of Eleven Locations:	0.0042 nm
Standard Deviation of the Mean:	0.00127 nm

Table VI. Uncertainty Budget for the 70 nm grating pitch measurement using the LRM-AFM at NMC/A*STAR.

	Quantity X_i	Relative Standard Uncertainty	Probability Distribution	Sensitivity Coefficient c_i	Standard Uncertainty $u_i(P)$ (nm)	Degrees of Freedom ν_i
Type A						
1	Measurement repeatability, R	—	N	—	0.00127	10
Type B						
2	Interferometer data (non-linearity, resolution) ΔN	0	—	—	Included in type A term due to averaging	—
3	Vacuum frequency, f_0	1.15×10^{-8}	R	70 nm	8.1×10^{-7}	∞
4	Refractive index of Air, n	7.1×10^{-7}	N	70 nm	4.97×10^{-5}	∞
5	Cosine error, θ_m	2.0×10^{-4}	R	70 nm	0.014	∞
6	Cosine error, θ_t	2.0×10^{-6}	R	70 nm	0.00014	∞
7	Cosine error, θ_O	3.9×10^{-10}	R	70 nm	2.7×10^{-8}	∞
8	Abbe error, L_{Abbe1}, (rotation around z-axis)	1.0×10^{-6}	R	70 nm	7.0×10^{-5}	∞
9	Abbe error, L_{Abbe2} , (rotation around y-axis)	1.0×10^{-6}	R	70 nm	7.0×10^{-5}	∞
10	Dead path, L_{dp}	0	—	—	Included in type A term due to averaging	—
11	Thermal expansion correction of metrology frame and corner mirror, L_{mf}	1.2×10^{-9}	R	70 nm	8.4×10^{-8}	∞
12	Thermal expansion of sample, L_{ms}	1.8×10^{-7}	R	70 nm	1.26×10^{-5}	∞
Combined Standard Uncertainty (k = 1)					0.014	∞
Expanded Uncertainty (k = 2)					0.028	∞

4.3.1 Uncertainties in NMC/A*STAR Measurements

The standard uncertainty evaluated as type A is obtained from a series of measurements on the repeatability and stability of the system. Based on a set of eleven measurement results as shown in table V above, the type A uncertainty of the system, measurement at the nominal pitch (70 nm) due to random effects was found to be less than 0.00127 nm.

The type B uncertainties for the NMC/A*STAR measurements are shown in table VI above. In most cases, a rectangular distribution with the limits stated was used to determine the standard uncertainty component for each effect. Most of the contributions are seen to be negligible.

The largest uncertainty contribution is due to the cosine error arising from potential misalignment of the interferometer axis with the mirror normal. This is followed by the type A contribution, and then the cosine error contribution arising from misalignment of the motion and measurement axes.

4.4 Summary and Comparison

The final results and uncertainties of the three participants are shown in table VII. The expanded uncertainties of the participants are comparable and the results are in agreement within these uncertainties.

Table VII. Comparison of pitch measurements and expanded uncertainties on the 70 nm grating.

Lab	Mean Pitch (nm)	Expanded Uncertainty (nm)
ASM (2 runs)	70.080	0.016
NIST	70.055	0.027
NMC	70.072	0.028

All three participants simultaneously measured and retained a specimen similar to the one used in the comparison, so as to preserve a basis for future improvements. While the offsets observed among the laboratories are within the uncertainties of the comparison, the differences are interesting and will be a subject of further investigation by the participants.

5. CONCLUSIONS

NIST, ASM, and NMC/A*STAR have completed a three-way interlaboratory comparison of traceable AFM pitch measurements on a 70 nm pitch grating. The three participants achieved relative expanded uncertainties (k = 2) of approximately 4×10^{-4} and their results were in agreement within the uncertainties.

The NIST and NMC/A*STAR results generally demonstrate what can accomplished in this size regime using instruments with integrated traceable interferometric displacement metrology. Both labs believe that the performance levels of their instruments can be further improved by at least a factor of two. In contrast, the ASM results illustrate that a commercially available AFM can be used to achieve uncertainties at the same level or, in this case, surpassing the performance of the metrology instruments used by NMIs. However, this approach requires a reference grating on which independent traceable measurements have been performed. In turn, this could be the province of instruments such as the C-AFM at NIST or the LRM-AFM at NMC/A*STAR. All three laboratories are working to further improve their capabilities and refine their uncertainty budgets.

ACKNOWLEDGEMENTS

This work was supported in part by the NIST Office of Microelectronics Programs and the Precision Engineering Division within the NIST Manufacturing Engineering Laboratory (MEL), the management of NMC/A*STAR, and internal research funds of ASM.

*Address all correspondence to Ronald Dixson at ronald.dixson@nist.gov

REFERENCES

1. R. Dixson, N. G. Orji, J. Fu, M. Cresswell, R. Allen, W. Guthrie, "Traceable Atomic Force Microscope Dimensional Metrology at NIST," *SPIE Proceedings* Vol. **6152**, 61520P-1-11 (2006).

2. D. A. Chernoff, E. Buhr, D. Burkhead, A. Diener, "Picometer-scale accuracy in pitch metrology by optical diffraction and atomic force microscopy," *SPIE Proceedings* Vol. **6922**, 69223J-1 (2008).

3. S. H. Wang, G. Xu and S. L. Tan, "Development of a metrological atomic force microscope for nano-scale standards calibration," *SPIE Proceedings,* Vol. **7155**, pp. 71550I.1-71550I.8 (2008).

4. J. A. Kramar, R. Dixson, N. G. Orji, "Scanning Probe Microscope Dimensional Metrology at NIST," submitted to *Meas. Sci. Technol.* (2010).

5. R. Dixson, R. Köning, V.W. Tsai, J. Fu, T.V. Vorburger, "Dimensional Metrology with the NIST calibrated atomic force microscope," *SPIE Proceedings* Vol. **3677**, 20-34 (1999).

6. R. Dixson, R. Köning, T. V. Vorburger, J. Fu, V. W. Tsai, "Measurement of pitch and width samples with the NIST calibrated atomic force microscope," *SPIE Proceedings* Vol. **3332**, 420-432 (1998).

7. *Guide to the Expression of Uncertainty in Measurement*, International Organization for Standardization, Geneva (1995).

8. B. N. Taylor and C. E. Kuyatt, *Guidelines for Evaluating and Expressing the Uncertainty of NIST Measurement Results*, NIST Tech. Note 1297, (1994).

9. Donald A. Chernoff and David L. Burkhead, "Automated, high precision measurement of critical dimensions using the Atomic Force Microscope," *J. Vac. Sci. Technol. A* Vol. **17**, 1457-1462 (1999).

10. Donald A. Chernoff and Jason D. Lohr, "High precision calibration and feature measurement system for a scanning probe microscope," U.S. Patent # 5,644,512 (1997).

11. Chernoff, D. A. and Lohr, J. D., "High precision calibration and feature measurement system for a scanning probe microscope," U.S. Patent 5825670, (1998).

12. G. Barrie Wetherill, *Elementary Statistical Methods,* (Methuen & Co., London, 1967), pp.263 ff.